AC

BCCNT 96/122/260

Dispersion Relations for Correlated Two-Pion Exchange in a Quark-Quark Scattering Amplitude

L.S. Celenza, Xiang-Dong Li, and C.M. Shakin

Department of Physics and Center for Nuclear Theory

Brooklyn College of the City University of New York

Brooklyn, New York 11210

(December, 1996)

Submitted to Physical Review C (Subnucleon Aspects of Nuclei/Physics of Hadrons)

Abstract

We study t-channel correlated two-pion exchange in a quark-quark scattering amplitude, $t_{qq}(q^2)$. (Since we use a generalized Nambu−Jona-Lasinio model that includes a model of confinement, the scattering amplitude is only defined for off-mass-shell quarks.) We calculate $\mathrm{Im}\, t_{qq}(q^2)$ for scalar-isoscalar t-channel exchange and obtain $\mathrm{Re}\, t_{qq}(q^2)$ using a once-subtracted dispersion relation. For $q^2 \leq 0$, $\mathrm{Re}\, t_{qq}(q^2)$ may be approximated by $t_{qq}(q^2) = g^2/(q^2 - m_\sigma^2)$ with $m_\sigma \simeq 600$ MeV. However, there is no sigma meson with that mass in the timelike region, $q^2 > 0$. (The physical sigma has a mass of about 850 MeV and a very large width.) Instead of using the dispersion relation, we can perform an explicit calculation of $t_{qq}(q^2)$ over the full range of q^2. By comparing our explicit calculation to the results of the dispersion-relation analysis, we may understand the physical significance of the effective sigma field introduced in the dispersion-relation study. At the quark level, we see that the T matrix (for $q^2 \leq 0$) describes the t-channel exchange of the (off-mass-shell) chiral partner of the pion. We also find that our model is able to reproduce the strength of the nucleon-nucleon force due to sigma exchange, as given, for example, in the phenomenological one-boson-exchange model.

I. Introduction

It is well known that, if one studies dispersion relations for nucleon-nucleon scattering, correlated two-pion exchange plays an important role in providing the intermediate-range attraction of the *NN* interaction [1-4]. It has been determined that the dynamics of correlated two-pion exchange may be approximated by the t-channel exchange of an (effective) sigma meson with $m_\sigma \sim 600$ MeV. In our work we wish to study a similar problem in which we consider the quark-quark interaction instead of the nucleon-nucleon interaction. Our motivation is to provide a physical interpretation of the "scalar meson" that approximates the t-channel dynamics of correlated two-pion exchange between quarks for $q^2 \leq 0$. This analysis is possible, since we can solve for the quark-quark scattering amplitude, $t_{qq}(q^2)$, for both timelike and spacelike values of q^2. Therefore, by studying our explicit calculation of $t_{qq}(q^2)$ for $q^2 \leq 0$, we can see that the (effective) sigma meson, introduced in the dispersion relation study is an off-mass-shell representation of the chiral partner of the pion. In this manner we obtain a deeper understanding of the physics underlying the dispersion relation analysis and may relate that work to models of the *NN* interaction that are based on models with chiral symmetry.

The organization of our work is as follows. In Section II we review some features of our generalized Nambu−Jona-Lasinio model [5-7]. In our work, we have defined two functions, $\hat{J}_S(q^2)$ and $\hat{K}_S(q^2)$, which may be used to construct a quark-quark scattering amplitude describing scalar-isoscalar t-channel exchange processes. (We note that $\hat{J}_S(q^2)$ is real, while $\hat{K}_S(q^2)$ is complex.) In Section III, we define the amplitude $t_{qq}(q^2)$ in terms of $\hat{J}_S(q^2)$ and $\hat{K}_S(q^2)$. We then use $\mathrm{Im}\, t_{qq}(q^2)$ in Section IV to obtain $\mathrm{Re}\, t_{qq}(q^2)$ from a once-subtracted dispersion relation. It is found that the approximation $t_{qq}(q^2) \simeq g^2_{\sigma qq}/(q^2 - m^2_\sigma)$,

with $m_\sigma = 600$ MeV, is valid in a limited region of spacelike values of q^2 near $q^2 = 0$. Finally, Section V contains a discussion of the significance of our result in understanding the nature of correlated two-pion exchange.

II. A Generalized Nambu−Jona-Lasinio Model

Our analysis of a generalized Nambu−Jona-Lasinio model [5-7] is reviewed in this section. The Lagrangian of the model is

$$\mathcal{L} = \bar{q}(x)(i\partial\!\!\!/ - m_q^0)q(x) + \frac{G_S}{2}\left[(\bar{q}(x)q(x))^2 + (\bar{q}(x)i\gamma_5\vec{\tau}q(x))^2\right] + \mathcal{L}_{\rm conf} \quad , \tag{2.1}$$

where $q(x)$ the quark field. Here m_q^0 is the current quark mass and $\mathcal{L}_{\rm conf}$ represents our model of confinement. (We will not discuss the details of our model of confinement, which have been given elsewhere [5,6]. Our confinement model is based upon the use of a linear potential; however, we carry out our analysis in momentum space using the Fourier transform of the potential [5-7].) To proceed, we need to define several integrals. For example, the quark-loop integral of Fig. 1b defines a function

$$-iJ_S(q^2) = (-1)n_f n_c \int \frac{d^4k}{(2\pi)^4} {\rm Tr}\left[iS(k+q/2)iS(k-q/2)\right] \tag{2.2}$$

where $S(k) = [k\!\!\!/ - m_q + i\epsilon]^{-1}$ is the quark propagator. In Fig. 1c we show the sum of a "ladder" of confining interactions, V^C, that serves to define a confinement vertex (the shaded triangular area). It is useful to introduce

$$-i\hat{J}_S(q^2) = n_f n_c \int \frac{d^4k}{(2\pi)^4} {\rm Tr}\left[S(k+q/2)\Gamma_S(q,k)S(k-q/2)\right] \quad , \tag{2.3}$$

where $\Gamma_S(q,k)$ is the confining vertex. [See Fig. 1c.]

In Fig. 1d we exhibit the function $K_S(q^2)$, which is important in the description of the coupling of the quark states to the two-pion continuum. In Fig. 1e we show the same function including the confining vertex. The vertex, $\Gamma_S(q,k)$, vanishes when both the quark and antiquark go on their positive mass shells [6]. Therefore, unitarity cuts that would start at

$4m_q^2$ are eliminated, leaving only the cut in $\hat{K}_S(q^2)$ that starts at $4m_\pi^2$. It is that feature that allows us to write meaningful dispersion relations.

Note that, in the absence of confinement, the mass of the sigma meson may be obtained from the equation

$$G_S^{-1} - J_S(m_\sigma^2) = 0 \quad . \tag{2.4}$$

The NJL model predicts a sigma meson with $m_\sigma^2 = 4m_q^2 + m_\pi^2$ [8]. We have used $m_q = 260$ MeV in our work and have, therefore, found $m_\sigma = 540$ MeV. In the presence of confinement, and including some effects due to the coupling to the two-pion states, we use

$$G_S^{-1} - \left[\hat{J}_S(m_\sigma^2) + \mathrm{Re}\,\hat{K}_S(m_\sigma^2)\right] = 0 \tag{2.5}$$

to determine the sigma mass. The last equation yields $m_\sigma = 823$ MeV [9]. However, since $\mathrm{Im}\,\hat{K}_S(q^2)$ is very large, the state at 823 MeV has a very large width of about 1 GeV and will not figure prominently in any experiment. (This analysis and the work of Törnqvist and Roos [10] show that the physical sigma has a mass of about 850 MeV and a very large width. The pole associated with this physical state does not influence the behavior of $t_{qq}(q^2)$ for spacelike q^2, where the effective mass is smaller [5]. Consideration of confinement and the coupling to the two-pion states can move the effective value for $q^2 < 0$ to 600 MeV.)

Values of $\mathrm{Im}\,\hat{K}_S(q^2)$ and $\mathrm{Re}\,\hat{K}_S(q^2)$ are shown in Figs. 2 and 3 [9]. In Fig. 4 we show values of $\hat{J}_S(q^2)$ for $q^2 > 0$, as well as $\hat{J}_S(q^2) + \mathrm{Re}\,\hat{K}_S(q^2)$ [9]. We may solve Eq. (2.5) in a graphical manner by drawing a horizontal line representing G_S^{-1}. The intersection of that line with the curve representing $\hat{J}_S(q^2) + \mathrm{Re}\,\hat{K}_S(q^2)$ provides a value for the physical sigma mass. [See Fig. 4.] (In our earlier work, we found $m_\sigma = 823$ MeV, as noted above.)

III. The Quark-Quark T Matrix

The functions defined in Section II may be used to construct a quark-quark T matrix, $t_{qq}(q^2)$, describing scalar-isoscalar exchange dynamics in the t-channel. (In this analysis we suppress reference to Dirac and isospin matrices. For the case considered here, only the unit matrices are needed in each space.) The expression for $t_{qq}(q^2)$, taking into account the processes shown in Fig. 5, is

$$t_{qq}(q^2) = -\frac{G_S}{1 - G_S\left[\hat{J}_S(q^2) + \hat{K}_S(q^2)\right]} \tag{3.1}$$

$$= -\frac{G_S}{1 - G_S\left[\hat{J}_S(q^2) + \mathrm{Re}\,\hat{K}_S(q^2)\right] - iG_S\mathrm{Im}\,\hat{K}_S(q^2)} \quad . \tag{3.2}$$

Note that, in the standard counting of color factors, $G_S \sim 1/n_c$ and $\hat{J}_S(q^2) \sim n_c$, while $\hat{K}_S(q^2) \sim 1$. Thus, $t_{qq}(q^2)$ is of order $1/n_c$, when we consider only the Born term shown in Fig. 1a and diagrams with various factors of $\hat{J}_S(q^2)$. On the other hand, adding a single factor of $\hat{K}_S(q^2)$ in a diagram contributing to $t_{qq}(q^2)$ gives a contribution of order $1/n_c^2$. (Also, Born terms involving uncorrelated exchange of two pions would give contributions of order $1/n_c^2$. These terms do not contribute to correlated two-pion exchange and we do not evaluate them here.)

It is useful to define

$$D(q^2) = 1 - G_S\left[\hat{J}_S(q^2) + \mathrm{Re}\,\hat{K}_S(q^2)\right] - iG_S\mathrm{Im}\,\hat{K}_S(q^2) \quad . \tag{3.3}$$

Thus,

$$\mathrm{Im}\, t_{qq}(q^2) = -\frac{G_S^2 \mathrm{Im}\, \hat{K}_S(q^2)}{|D(q^2)|^2} \quad . \tag{3.4}$$

Various diagrams that contribute to $\mathrm{Im}\, t_{qq}(q^2)$ are shown in Fig. 6. We may also write

$$\mathrm{Im}\, t_{qq}(q^2) = \sum_{ab} \frac{s}{2} \int \frac{d^4\kappa}{(2\pi)^4} T^{ab}_{q\pi}(q,\kappa) \Big[i^2 (-2\pi i) \delta^{(+)}\big((q/2+\kappa)^2 - m_\pi^2\big) \times (-2\pi i) \delta^{(+)}\big((q/2-\kappa)^2 - m_\pi^2\big) \Big] \Big[T^{ab}_{q\pi}(q,\kappa) \Big]^\dagger \quad , \tag{3.5}$$

thereby defining the amplitude $T^{ab}_{q\pi}(q,\kappa)$. Note that $s=2$ is a symmetry factor and we divide by 2 to relate the discontinuity to the imaginary part of $t_{qq}(q^2)$. [See Fig. 6b.] In Eq. (3.5), a and b are isospin indices. The intermediate bracketed quantity arises when forming the discontinuity across the cut that starts at $q^2 = 4m_\pi^2$. (There is one factor of i from each meson propagator.)

It is useful to define the form factor $F_1(q^2)$ shown in Fig. 7. In this case, the pions have been placed on mass shell. That feature is denoted by placing a cross on each of the pion lines. The function $F_1(q^2)$ may be obtained from the more general amplitude

$$\mathscr{F}_S(q,\kappa) = \mathrm{Tr} i \int \frac{d^4k}{(2\pi)^4} \big[S(k-\kappa)\gamma_5 S(q/2+k) \Gamma_S(q,k) S(-q/2+k)\gamma_5 \big] \tag{3.6}$$

by taking $(q/2+\kappa)^2 = m_\pi^2$ and $(q/2-\kappa)^2 = m_\pi^2$, etc. That is,

$$F_1(q^2) = \mathscr{F}_S \left[q^2, q\cdot\kappa = 0, \kappa^2 = \frac{q^2}{4} - m_\pi^2 \right] \quad . \tag{3.7}$$

Further details concerning the calculation of $F_1(q^2)$ may be found in Ref. [9].

If $\vec{q} = 0$, we have $q^0 = 2\omega(\vec{\kappa})$, with $\omega(\vec{\kappa}) = [\vec{\kappa}^2 + m_\pi^2]^{1/2}$. We may then provide an expression for $T^{ab}_{q\pi}(q^2)$ in terms of $F_1(q^2)$ in the case of on-mass-shell pions:

$$T^{ab}_{q\pi}(q^2) = \delta_{ab} n_c n_f \frac{g^2_{\pi qq} G_S F_1(q^2)}{D(q^2)} \quad . \tag{3.8}$$

Here $n_f = 2$ and $n_c = 3$ are the number of flavors and colors, respectively. Note that in $\mathrm{Im}\, t_{qq}(q^2)$, the <u>total</u> isospin factor is $3n_f^2 = 12$ and the color factor is $n_c^2 = 9$.

IV. Dispersion Relations for the Quark-Quark Scattering Amplitude

A once-subtracted dispersion relation for $\mathrm{Re}\, t_{qq}(q^2)$ is

$$\mathrm{Re}\, t_{qq}(q^2) = t_{qq}(0) - \frac{P}{\pi} q^2 \int_{4m_\pi^2} \frac{\mathrm{Im}\, t_{qq}(q'^2)}{q'^2(q^2 - q'^2)} dq'^2 \quad . \tag{4.1}$$

In analogy to what is done in the study of the *NN* scattering amplitude [1-4], we insert our model for $\mathrm{Im}\, t_{qq}(q'^2)$ in Eq. (4.1). [See Eq. (3.4).] We show $\mathrm{Im}\, t_{qq}(q^2)$ in Fig. 8 along with the values of $\mathrm{Re}\, t_{qq}(q^2)$ obtained from Eq. (4.1). In order to carry out that calculation we have used

$$t_{qq}(0) = - \frac{G_S}{1 - G_S\left[\hat{J}_S(0) + \hat{K}_S(0)\right]} \tag{4.2}$$

in Eq. (4.1). (We find that $t_{qq}(0) = -27.9\ \mathrm{GeV}^{-2}$.)

It may be seen that the values of $\mathrm{Re}\, t_{qq}(q^2)$ obtained from Eq. (4.1) agree well with those found in an explicit calculation using Eq. (3.2). We have proceeded in this fashion to make our treatment of correlated two-pion exchange similar to that used in the study of nucleon-nucleon scattering [1-4]. We come to the same conclusion. If we consider spacelike values of q^2, the contribution of correlated two-pion exchange may be replaced by the exchange of an effective sigma meson of mass $m_\sigma \sim 600$ MeV.

However, our analysis allows us to go further in understanding the dynamics for spacelike q^2. Since $\hat{K}_S(q^2)$ is not very important for $q^2 \leq 0$, we may write

$$t_{qq}(q^2) \simeq - \frac{G_S}{1 - G_S \hat{J}_S(q^2)} \quad . \tag{4.3}$$

Also, since confinement is also not very important in the spacelike domain we can further

approximate $t_{qq}(q^2)$ by

$$t_{qq}(q^2) \simeq -\frac{G_S}{1 - G_S J_S(q^2)} \quad . \tag{4.4}$$

As we may see in Fig. 8,

$$t_{qq}(q^2) \simeq \frac{g^2_{\sigma qq}}{q^2 - m^2_\sigma} \quad , \tag{4.5}$$

with $g_{\sigma qq}$ a constant, for $-q^2$ not too large. (For example, $-0.20\ \text{GeV}^2 < q^2 < 0$.)

It should be clear that Eq. (4.5) describes the exchange of the chiral partner of the pion between the quarks, with a coupling constant of the meson to the quark of $g_{\sigma qq}$. Recall that, if we neglect confinement and use Eq. (4.4) in the timelike region, we obtain 540 MeV for the mass of the chiral partner of the pion. That agrees with the bosonization analysis, which yields $m^2_\sigma = 4m^2_q + m^2_\pi$ [8]. Inclusion of confinement and coupling to the two-pion states leads to an effective mass $m_\sigma = 600$ MeV in the spacelike region, and $m_\sigma = 823$ MeV for the mass of the physical sigma meson. [See Fig. 8.]

For a more accurate analysis we may use

$$t_{qq}(q^2) = -\frac{G_S}{1 - G_S\left[\hat{J}_S(q^2) + \text{Re}\,\hat{K}_S(q^2)\right]} \tag{4.6}$$

for $q^2 < 0$. We may also define a momentum-dependent coupling parameter, $g_{\sigma qq}(q^2)$, such that

$$\frac{g^2_{\sigma qq}(q^2)}{q^2 - m^2_\sigma} = -\frac{G_S}{1 - G_S\left[\hat{J}_S(q^2) + \text{Re}\,\hat{K}_S(q^2)\right]} \quad . \tag{4.7}$$

We may then define $g_{\sigma qq} = g_{\sigma qq}(0)$. To obtain a value for $g_{\sigma qq}$, we use the relation

$$\frac{G_S}{1 - G_S\left[\hat{J}_S(0) + \hat{K}_S(0)\right]} = \frac{g^2_{\sigma qq}}{m^2_\sigma} \quad . \tag{4.8}$$

With $m_\sigma = 540$ MeV, $\hat{J}_S(0) = 0.0708$ GeV^2, $\hat{K}_S(0) = 0.0108$ GeV^2 and $G_S = 8.516$ GeV^2, we find $g_{\sigma qq} = 2.85$ [9]. (Note that, if we use $m_\sigma = 600$ MeV, we would find $g_{\sigma qq} = 3.17$.) These values yield $t_{qq}(0) = -g^2_{\sigma qq}/m^2_\sigma = -27.9$ GeV^{-2}.

Once we have a value of $g_{\sigma qq}$, we can compare the strength of the interaction between nucleons in our quark model and in the one-boson-exchange (OBE) model of nuclear forces [11]. To make that comparison at $q^2 = 0$, we need the value of the scalar form factor of the nucleon defined for valence quarks. (That quantity has been calculated in a lattice simulation of QCD [12].) We define the scalar form factor that has contributions from both the valence and "sea" quarks, as

$$F_S(q^2)\bar{u}(\vec{p}+\vec{q}, s')u(\vec{p}, s)\delta_{\tau\tau'} = \langle \vec{p}+\vec{q}, s', \tau' \,|\, \bar{q}(0)q(0) \,|\, \vec{p}, s, \tau \rangle \quad . \tag{4.9}$$

Here, s, s', τ, τ' are spin and isospin indices. It is found that $F_S(q^2)$ is about three times as large as the valence form factor, which we denote as $F_S^{val}(q^2)$ [12]. At $q^2 = 0$, the sigma-nucleon coupling constant in our quark model is $G_{\sigma NN} = g_{\sigma qq} F_S^{val}(0)$ [13]. From the lattice simulation [12], we have $F_S^{val}(0) = 3.02$, so that with $g_{\sigma qq} = 2.85$, we have $G_{\sigma NN} = 8.61$. To obtain the corresponding coupling constant for the OBE model, $G^{OBE}_{\sigma NN}$, we recall that there a vertex cutoffs in that model [11], so that, with $g^2_{\sigma NN}$ being the OBE coupling constant, we have (for $q^2 = 0$)

$$\frac{\left(G_{\sigma NN}^{OBE}\right)^2}{m_\sigma^2} = \frac{g_{\sigma NN}^2}{\tilde{m}_\sigma^2}\left[\frac{\Lambda_\sigma^2 - \tilde{m}_\sigma^2}{\Lambda_\sigma^2}\right]^2 . \tag{4.10}$$

Here, $\tilde{m}_\sigma = 550$ MeV is the value of the sigma mass usually used in the OBE model, $g_{\sigma NN}$ is the OBE coupling constant, and Λ_σ is the corresponding vertex cutoff parameter. For one particular OBE model, we have $g_{\sigma NN}^2/4\pi = 8.314$ and $\Lambda_\sigma = 2.0$ GeV. (See Table A.2 of reference [11].) Therefore, we find $G_{\sigma NN}^{OBE} = 9.28$ from Eq. (4.10) if we put $m_\sigma = 540$ MeV.

The ratio of the value calculated above, $G_{\sigma NN} = 8.61$, to the effective value in the OBE model, $G_{\sigma NN}^{OBE} = 9.28$, is 0.928. Thus we see that our model can account for at least eighty-five percent of the nucleon-nucleon force that is described as being due to sigma exchange in the OBE model [11]. (If we use $m_\sigma = 600$ MeV in Eq. (4.10), we have $G_{\sigma NN}^{OBE} = 10.3$. Also, when $m_\sigma = 600$ MeV, we have $g_{\sigma qq} = 3.17$ and $G_{\sigma NN} = g_{\sigma qq} F_S(0) = 9.57$. Therefore, $G_{\sigma NN}^{OBE} / G_{\sigma NN}^{OBE} = 1.08$. With that choice of m_σ, we can account for the entire strength of the scalar-isoscalar interaction at $q^2 = 0$.)

V. Discussion

Our goal in this paper was to relate the description of correlated two-pion exchange in the nucleon-nucleon interaction [1-4] to a similar description for the quark-quark interaction. The advantage of studying the problem at the quark level is that one may specify the chiral character of the fields involved. If one studies the nucleon-nucleon interaction, the nature of the effective sigma field, introduced to represent correlated two-pion exchange, is unknown. Working at the quark level, it is clear that, for spacelike q^2, the exchanged scalar-isoscalar meson is the (off-mass-shell) chiral partner of the pion. If we infer that a similar interpretation may be made for the scalar field that simulates correlated two-pion exchange in the nucleon-nucleon interaction, we achieve a more comprehensive and unified understanding of that interaction. We also achieve a greater understanding of the nature of scalar fields in nuclei [22-24].

Recent work on the nucleon-nucleon interaction has made use of effective Lagrangians that exhibit chiral symmetry, with mesons and nucleons as the degrees of freedom [14-21]. (Such models usually require a large number of free parameters. For example, there are 26 parameters in the work of Ref. [16].) While we have not introduced a Lagrangian with chiral symmetry, with mesons and nucleons as the degrees of freedom, we believe that our analysis, which is based on a model with chiral symmetry, with quarks as the basic degrees of freedom, is useful in understanding the role of chiral symmetry in the nucleon-nucleon interaction.

Acknowledgement

This work is supported in part by a grant from the National Science Foundation and by the PSC-CUNY Faculty Research Award Program of the City University of New York.

References

[1] G.E. Brown and A.D. Jackson, The Nucleon-Nucleon Interaction (North-Holland, Amsterdam, 1976).

[2] J.W. Durso, M. Saavela, G.E. Brown and B.J. Verwest, Nucl. Phys. A278, 445 (1977).

[3] J.W. Durso, A.D. Jackson, and B.J. Verwest, Nucl. Phys. A345, 471 (1980).

[4] W. Lin and B.D. Serot, Nucl. Phys. A512, 637 (1990).

[5] L.S. Celenza, Xiang-Dong Li, C.M. Shakin, and Wei-Dong Sun, Utility of the Linear Sigma Model for Scalar Mesons with Spacelike Momenta, Brooklyn College Report: BCCNT 96/111/258 (1996) – submitted for publication.

[6] L.S. Celenza, C.M. Shakin, Wei-Dong Sun, J. Szweda, and Xiquan Zhu, Phys. Rev. D51, 3638 (1995).

[7] L.S. Celenza, C.M. Shakin, Wei-Dong Sun, J. Szweda, and Xiquan Zhu, Intl. J. Mod. Phys. E2, 603 (1993).

[8] For reviews of the NJL model, see U. Vogl and W. Weise, Prog. Part. Nucl. Phys. 27, 195 (1951); S.P. Klevansky, Rev. Mod. Phys. 64, 649 (1992); T. Hatsuda and T. Kunihiro, Phys. Rep. 247, 223 (1994).

[9] L.S. Celenza, Xiang-Dong Li, and C.M. Shakin, Calculation of the Properties of the Sigma Meson in a Generalized NJL Model with Lorentz-Vector Confinement, Brooklyn College Report: BCCNT 96/121/259 (1996).

[10] N.A. Törnqvist and M. Roos, Phys. Rev. Lett. 76, 1575 (1996). These authors consider a quark model with unitary constraints and find $m_\sigma = 860$ MeV and $\Gamma_\sigma = 880$ MeV.

[11] R. Machleidt, in Advances in Nuclear Physics, edited by J.W. Negele and E. Vogt (Plenum, New York, 1988) Vol. 19.

[12] S.J. Dong, J.-F. Lagaë, and K.F. Liu, Phys. Rev. D54, 5496 (1996).

[13] C.M. Shakin and Wei-Dong Sun, Scalar-Isoscalar Meson Exchange in the Calculation of the Nucleon-Nucleon Interaction, Brooklyn College Report: BCCNT 96/041/255 (1996) - to be published in Physical Review C.

[14] L.S. Celenza, A. Pantziris, and C.M. Shakin, Phys. Rev. C46, 2213 (1992).

[15] C. Ordóñez, L. Ray, and U. van Kolck, Phys. Rev. Lett. 72, 1982 (1994).

[16] C. Ordóñez, L. Ray, and U. van Kolck, Phys. Rev. C53, 2086 (1996).

[17] S. Weinberg, Phys. Lett. B251, 288 (1990).

[18] S. Weinberg, Nucl. Phys. B363, 3 (1991).

[19] D.B. Kaplan, M.J. Savage, and M.B. Wise, Nucleon-Nucleon Scattering from Effective Field Theory, preprint: Inst. for Nuclear Theory, Univ. of Washington INT96-00-125 (1996).

[20] C.A. da Rocha and M.R. Robilotta, Phys. Rev. C52, 531 (1995).

[21] C.A. da Rocha and M.R. Robilotta, Phys. Rev. C49, 1818 (1994).

[22] L.S. Celenza, A. Pantziris, C.M. Shakin, and Wei-Dong Sun, Phys. Rev. C45, 2015 (1992).

[23] L.S. Celenza, A. Pantziris, C.M. Shakin, and Wei-Dong Sun, Phys. Rev. C46, 571 (1992).

[24] L.S. Celenza, C.M. Shakin, Wei-Dong Sun, and Xiquan Zhu, Phys. Rev. C48, 159 (1993).

Figure Captions

Fig. 1 (a) The zero-range quark interaction of the NJL model is shown.

(b) The quark-loop integral in the scalar-isoscalar channel is shown.

(c) The quark-loop integral including a series of confining interactions (dashed line) is shown. The filled triangular region denotes the vertex function that serves to sum the ladder of confining interactions.

(d) The function $K_S(q^2)$ describes effects of coupling to the two-pion continuum.

(e) The function $\hat{K}_S(q^2)$ includes two confinement vertex functions and has a cut for $q^2 > 4m_\pi^2$.

Fig. 2 Values of Im $\hat{K}_S(q^2)$ are shown. The calculation is made using the method outlined in Ref. [7]. Here we use $\kappa = 0.50$ GeV^2, $g_{\pi qq} = 2.58$ and Lorentz-vector confinement. We also have $m_q = 260$ MeV and a cutoff on the three-momenta, $|\vec{k}| \leq \Lambda_3$, with $\Lambda_3 = 0.689$ GeV. (Note that the result is quite insensitive to the model of confinement used.) Values for $g_{\pi qq} = 2.68$ may be obtained from the values shown by multiplying by $(2.68/2.58)^4 = 1.16$. [See Fig. 3.]

Fig. 3 Values of Re $\hat{K}_S(q^2)$ obtained in Ref. [9] are shown. Here $g_{\pi qq} = 2.68$ was used in the calculation of Im $\hat{K}_S(q^2)$ and Re $\hat{K}_S(q^2)$ was obtained using a once-subtracted dispersion relation.

Fig. 4 The dashed line shows Re $\hat{K}_S(q^2)$. [See Fig. 3.] The dotted line shows the values of $\hat{J}_S(q^2)$, and the solid line represents $\hat{J}_S(q^2)$ + Re $\hat{K}_S(q^2)$. These results were given in Ref. [9]. The dash-dot line shows the value of

$G_S^{-1} = (1/8.516)\ \text{GeV}^2$ [9]. The intersection of the solid line with the dash-dot line depicts the solution of the equation $G_S^{-1} - [J_S(q^2) + \text{Re}\,\hat{K}_S(m_\sigma^2)] = 0$. We find $m_\sigma = 823$ MeV.

Fig. 5 The quark-quark T matrix $t_{qq}(q^2)$ is obtained by summing the diagrams shown. The t-channel exchanges are summed by the expression given as Eq. 3.1. In a limited region of $q^2(-0.25\ \text{GeV}^2 < q^2 < 0)$, these effects are well represented by the exchange of an effective sigma meson with $m_\sigma = 600$ MeV, as may be seen in Fig. 8.

Fig. 6 (a) Some of the diagrams contributing to $\text{Im}\,t_{qq}(q^2)$ are shown. The wavy lines denote pions and the wavy lines with a cross represent on-mass-shell pions. [See Eq. (3.4).] To simplify the drawing, the confining vertex is not shown.

(b) A diagrammatic representation of Eq. (3.5) is shown. The wavy lines represent on-mass-shell pions.

Fig. 7 (a) The form factor, $F_1(q^2)$, is shown. The wavy lines represent pions and the crosses indicate that the pions are on-mass-shell. [See Eqs. (3.6) and (3.7).]

Fig. 8 The dashed line represents values of $\text{Im}\,t_{qq}(q^2)$, that were calculated by the methods described in the text. The solid line represents $\text{Re}\,t_{qq}(q^2)$, obtained using the once-subtracted dispersion relation of Eq. (4.1). Here $t_{qq}(0) = -27.9\ \text{GeV}^{-2}$ was obtained from Eq. (4.2). The dotted line represents the approximation, $t_{qq}(q^2) = g_{\sigma qq}^2/(q^2 - m_\sigma^2)$, with $m_\sigma = 600$ MeV and $g_{\sigma qq} = 3.17$.

iG_S

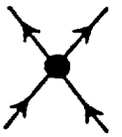

(a)

$-iJ_S(q^2) =$

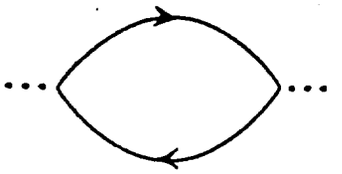

(b)

$-i\hat{J}_S(q^2) =$

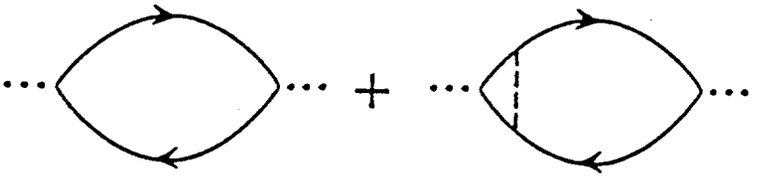

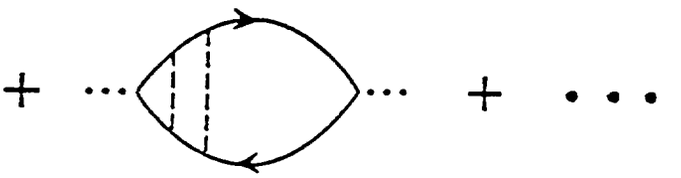

$=$

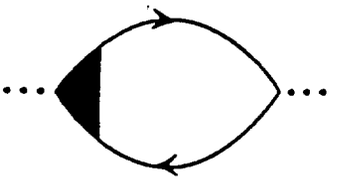

(c)

$-iK_S(q^2) =$

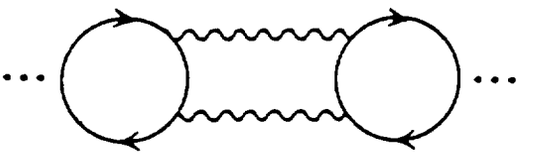

(d)

$-i\hat{K}_S(q^2) =$

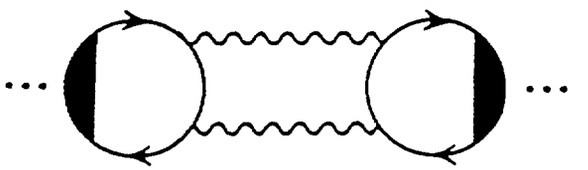

(e)

FIG. 1

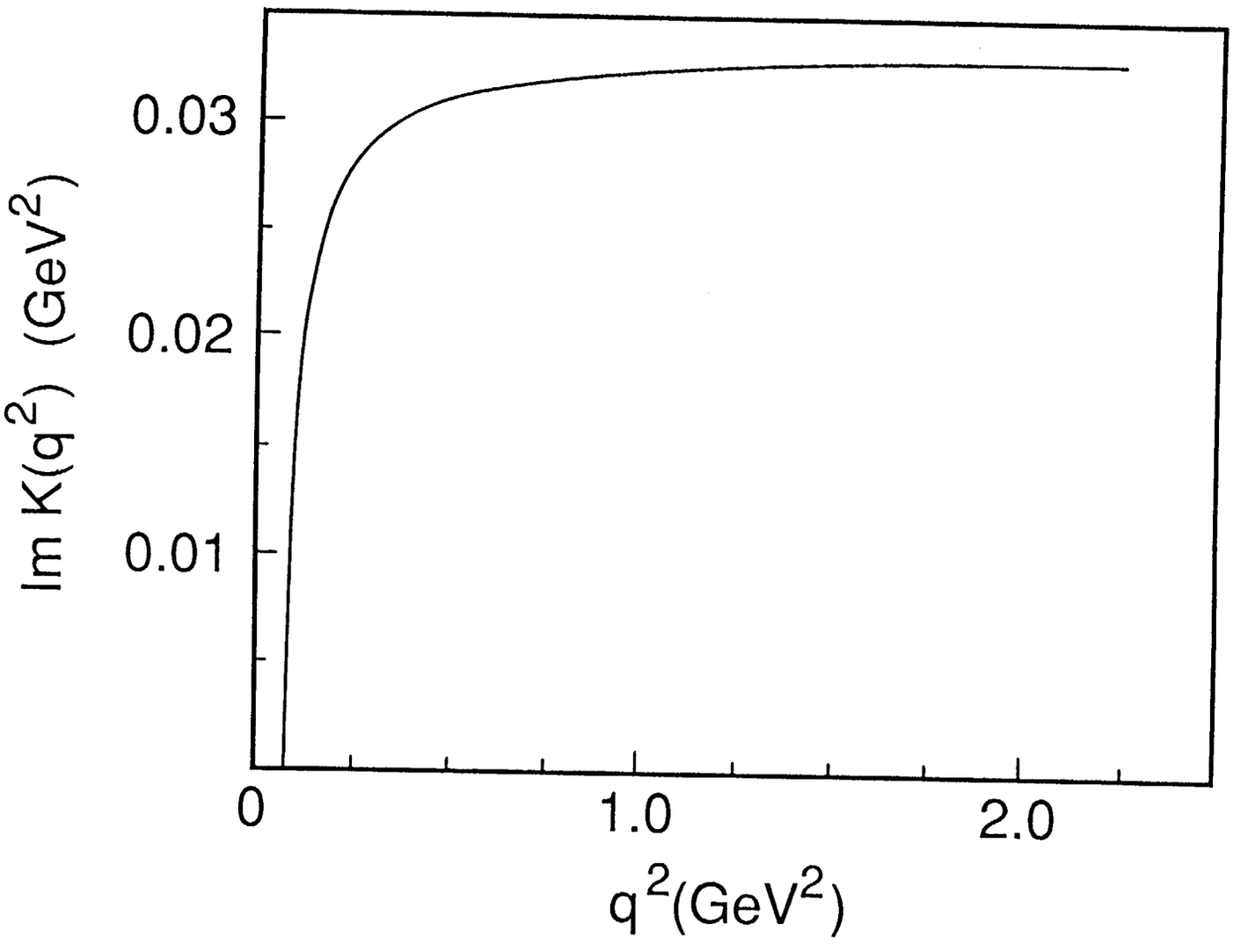

FIG. 2

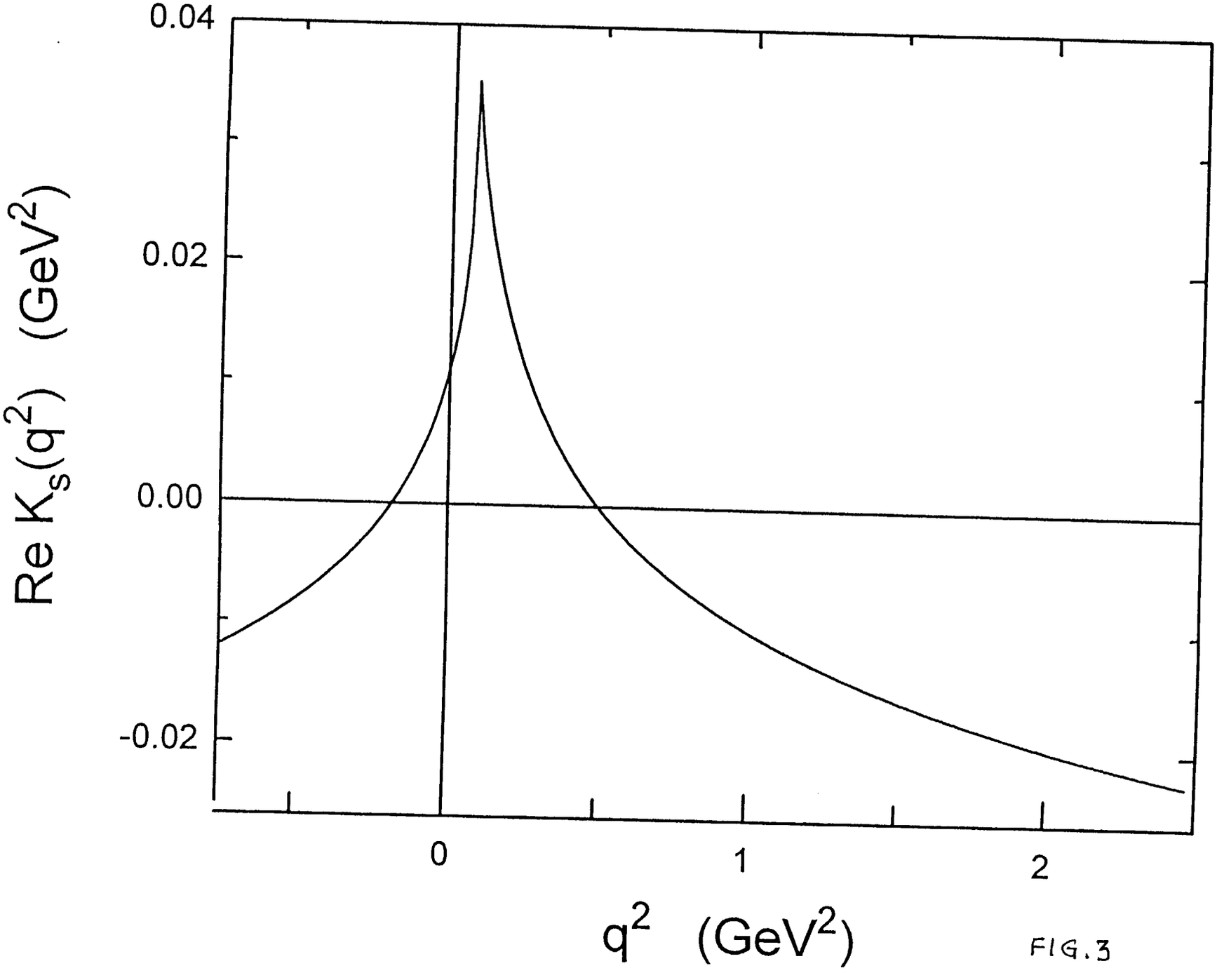

FIG. 3

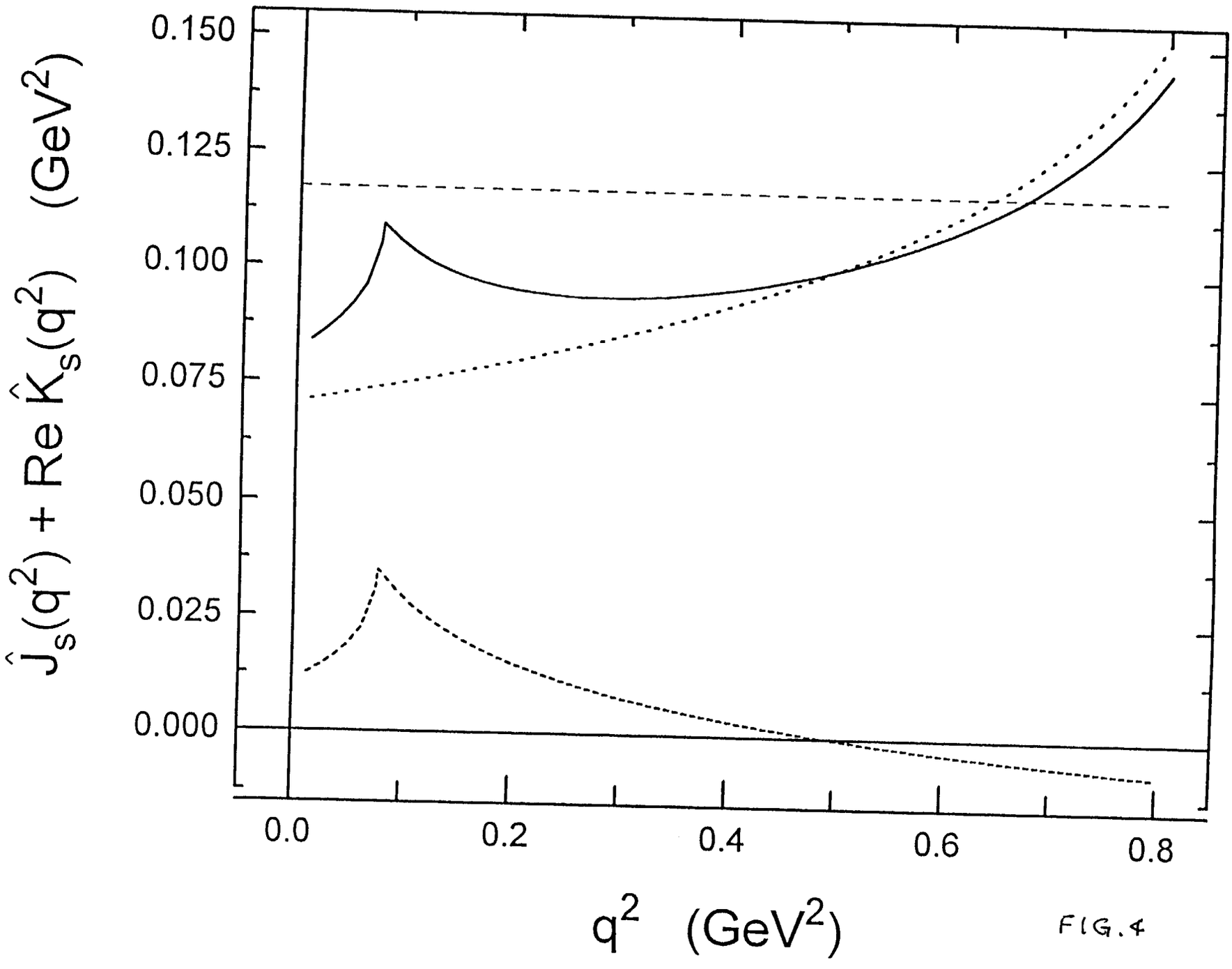
0.150
0.125
0.100
0.075
0.050
0.025
0.000
0.0
0.2
0.4
0.6
0.8
$\hat{J}_s(q^2) + \mathrm{Re}\,\hat{K}_s(q^2)$ (GeV^2)
q^2 (GeV^2)

FIG. 4

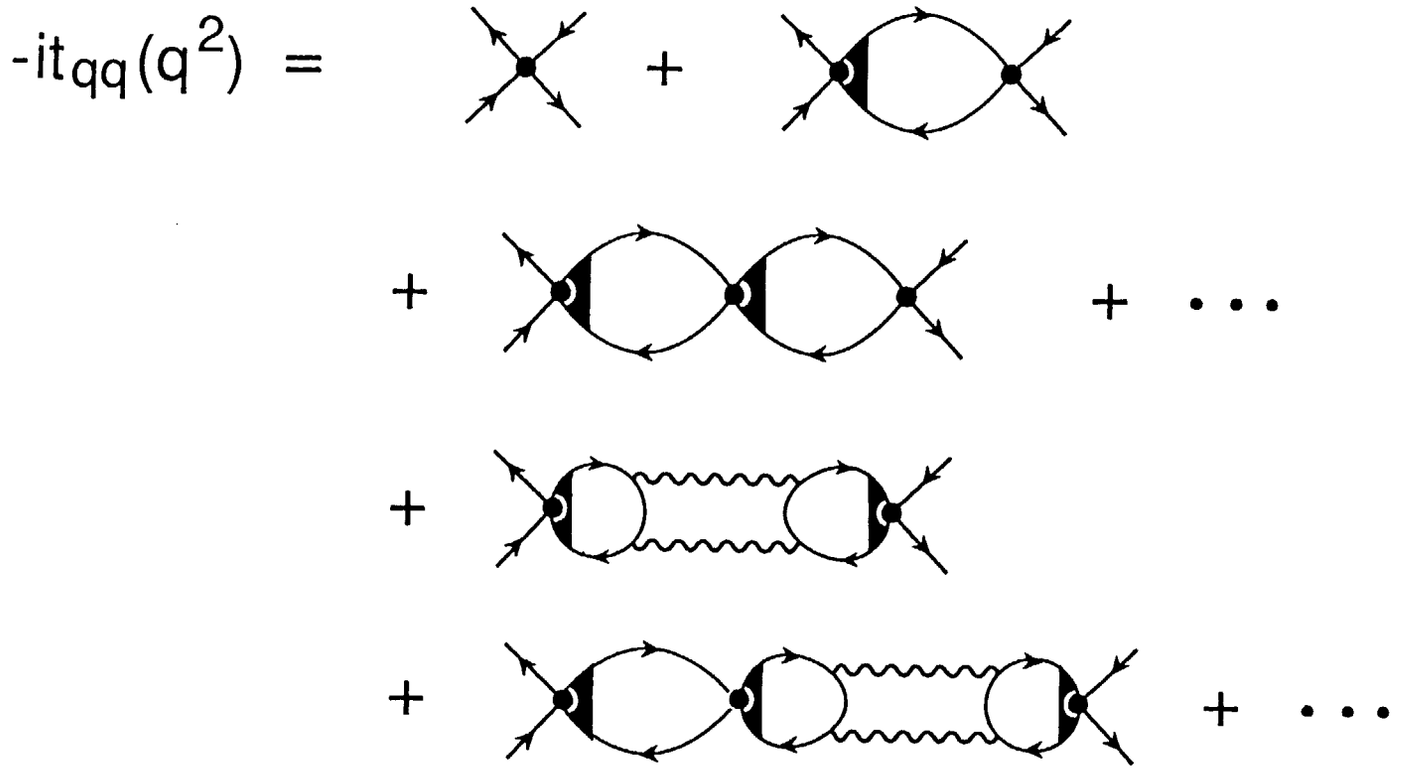

FIG. 5

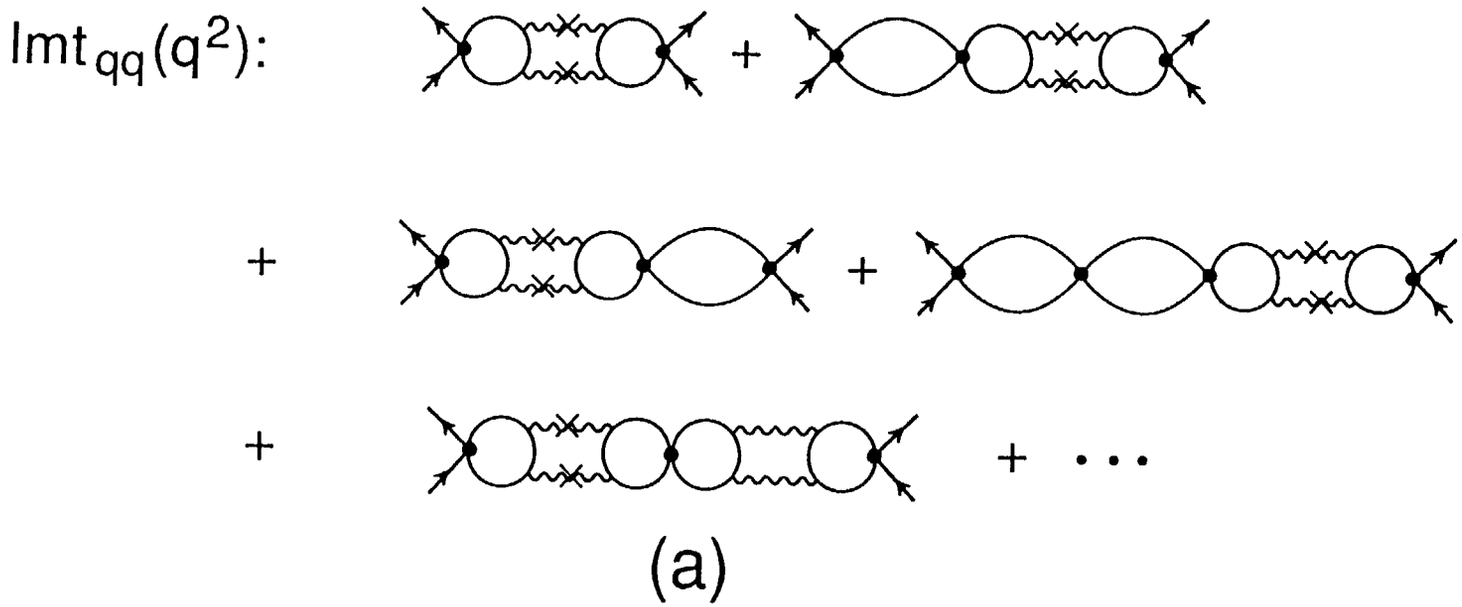
Imt$_{qq}(q^2)$:
+
+
+
+
+ ...
(a)

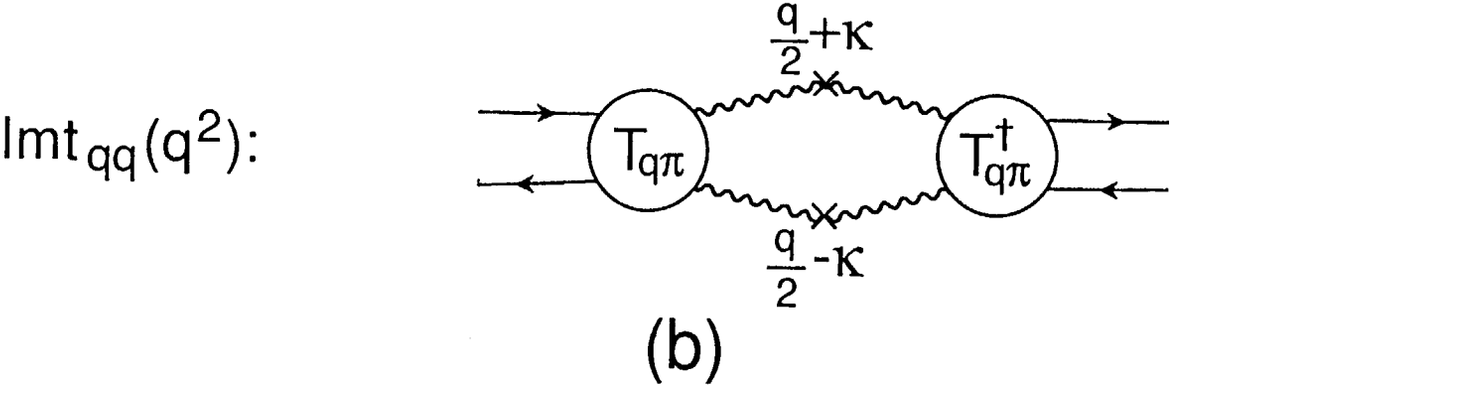
Imt$_{qq}(q^2)$:
$\frac{q}{2}+\kappa$
$T_{q\pi}$
$T^{\dagger}_{q\pi}$
$\frac{q}{2}-\kappa$
(b)

FIG. 6

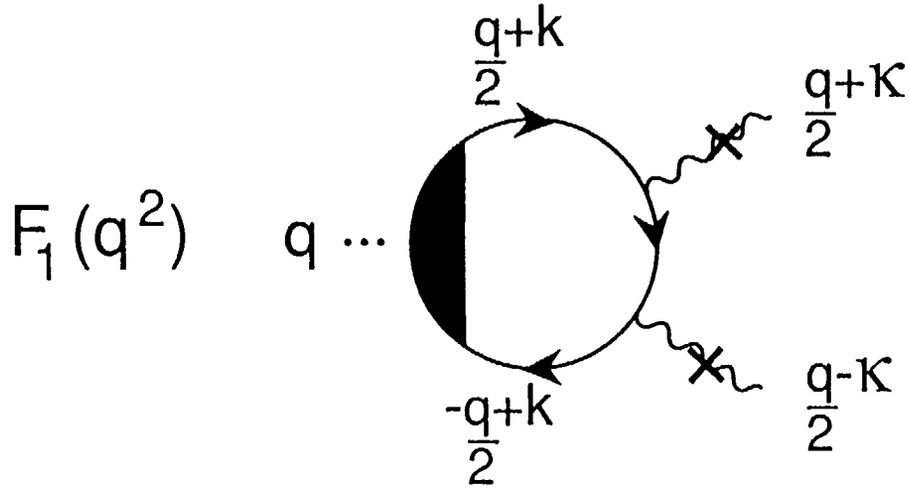

FIG.7

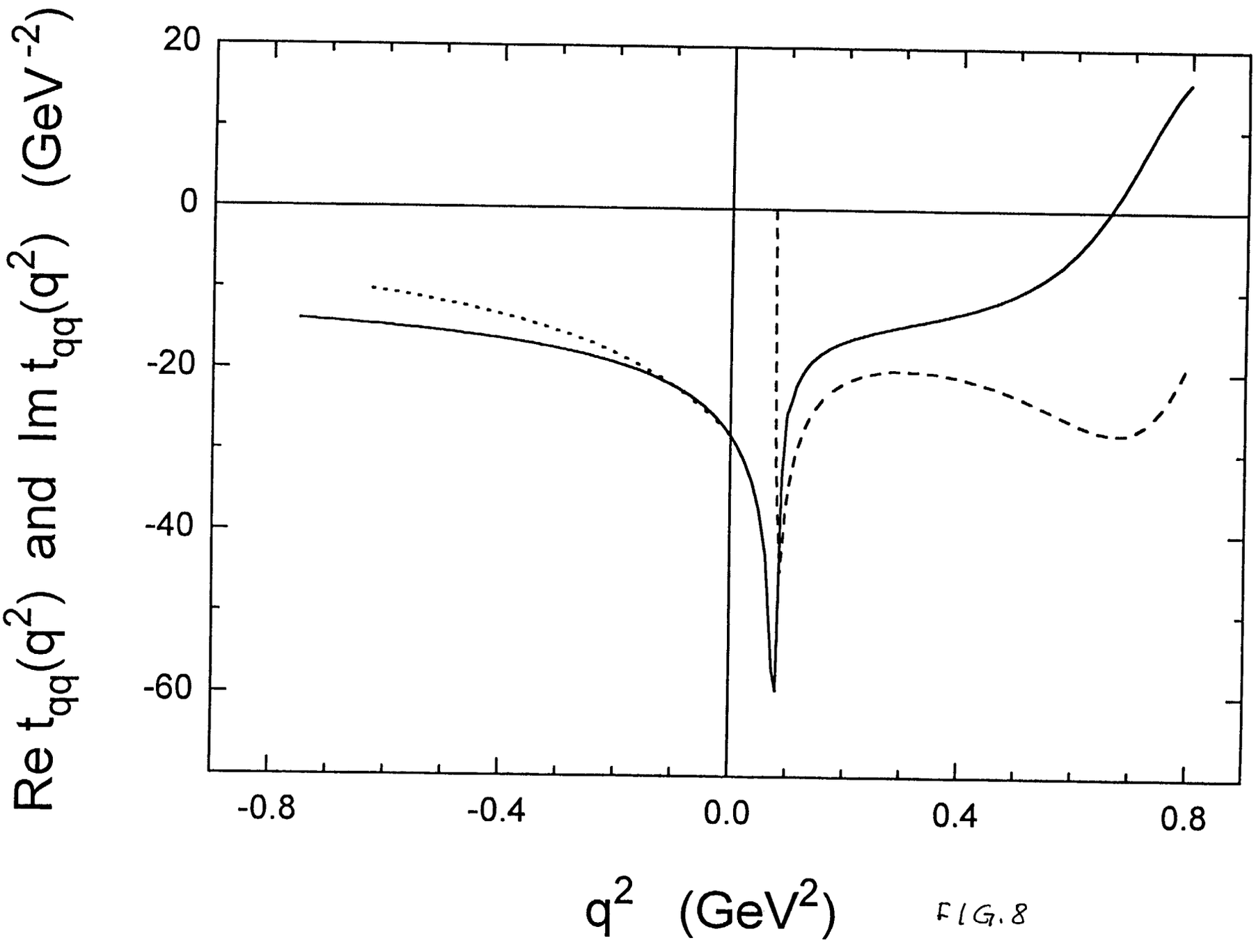

FIG. 8